

NJC

Accepted Manuscript



This is an *Accepted Manuscript*, which has been through the Royal Society of Chemistry peer review process and has been accepted for publication.

Accepted Manuscripts are published online shortly after acceptance, before technical editing, formatting and proof reading. Using this free service, authors can make their results available to the community, in citable form, before we publish the edited article. We will replace this *Accepted Manuscript* with the edited and formatted *Advance Article* as soon as it is available.

You can find more information about *Accepted Manuscripts* in the [Information for Authors](#).

Please note that technical editing may introduce minor changes to the text and/or graphics, which may alter content. The journal's standard [Terms & Conditions](#) and the [Ethical guidelines](#) still apply. In no event shall the Royal Society of Chemistry be held responsible for any errors or omissions in this *Accepted Manuscript* or any consequences arising from the use of any information it contains.



www.rsc.org/njc

ARTICLE

Enhanced catalytic activity of nanoporous $\text{Cu}_3(\text{BTC})_2$ metal-organic framework via immobilization of oxodiperoxo molybdenum complex

Cite this: DOI: 10.1039/x0xx00000x

Received 00th January 2012,
Accepted 00th January 2012

DOI: 10.1039/x0xx00000x

www.rsc.org/Sara Abednatanzi^a, Alireza Abbasi^a and Majid Masteri-Farahani^b

Molybdenum(VI) oxodiperoxo complex was immobilized into post synthetically modified $\text{Cu}_3(\text{BTC})_2$ metal-organic framework (abbreviated as CuBTC MOF, BTC = benzene-1,3,5-tricarboxylate). Characterization of the modified CuBTC MOF by Fourier transform infrared and atomic absorption spectroscopies as well as thermogravimetric and CHN elemental analyses confirmed successful modification of the framework. Powder X-ray diffraction revealed a shift for all peaks to smaller 2θ angles during the molybdenum complex attachment as the result of MOF expansion. Nitrogen adsorption/desorption techniques demonstrated a significant decrease in BET surface area and total pore volume during the modification process. The resulting molybdenum containing MOF showed higher catalytic activity and selectivity than the CuBTC MOF due to the presence of the molybdenum(VI) oxodiperoxo complex.

Introduction

In recent years, considerable efforts have been devoted to develop olefins epoxidation catalysts since epoxides are valuable intermediates in industries for the production of many fine chemicals such as polymers, surfactants and various pharmaceuticals [1].

Transition metal oxodiperoxo complexes have played an important role in the epoxidation of olefins [2-4]. Molybdenum(VI) oxodiperoxo complexes have been extensively applied as olefin epoxidation catalysts because of their high catalytic activity and selectivity under mild conditions [5]. In this regard, covalent attachment of these homogeneous molybdenum catalysts on insoluble solid supports has been the subject of great interest to increase catalyst stability and to facilitate post-reaction separation and recycling [6]. Although great attempts have been made to immobilize different molybdenum oxodiperoxo complexes on solid supports such as silica, Si-MCM-41 and Al-MCM-41 [6-11], these catalysts suffer from low loading and poor stability. In this concept, development of an ideal molybdenum catalyst that exhibits the best properties of both homogeneous and heterogeneous catalysts with high activity and stability still poses a considerable challenge.

Metal organic frameworks (MOFs) constructed from inorganic metal nodes and bridging organic linkers have opened new opportunities for application in the field of heterogeneous catalysis due to their microporosity, large specific surface area and especially their structural variety [12-14]. In recent years, post-synthetic modification (PSM) of MOFs has emerged as promising multifunctional materials to introduce a large variety of functional groups into the framework and design new heterogeneous catalysts

with enhanced catalytic efficiency [15-17]. Therefore, different active components have been employed to develop such heterogeneous oxidation catalysts including salen-Co(II) complex incorporated into NH_2 -MIL-101, manganese(III) porphyrin complex covalently attached to MIL-101, IRMOF-3 modified by manganese and vanadyl complexes [18-21]. However there are few reports on the attachment of effective molybdenum complexes using MOFs as porous supports through PSM process [22-23].

Among different utilized MOFs as solid supports in the preparation of heterogeneous oxidation catalysts, CuBTC is highly desirable because of its facile synthesis and activation, large specific surface area, relatively large cavities as well as persistence of microporosity even after solvent removal [24]. To the best of our knowledge there are few reports on the PSM of the CuBTC to prepare a heterogeneous epoxidation catalyst. Very recently we reported PSM of the CuBTC MOF through immobilization of bis(acetylacetonato)dioxomolybdenum(VI) as a heterogeneous epoxidation catalyst [25].

In the continuation of our research on the catalytic activity of heterogeneous molybdenum catalysts [25-27], we report an efficient approach to develop a new molybdenum-based heterogeneous catalyst using the CuBTC MOF as solid support. Covalent PSM of the CuBTC MOF was achieved by immobilizing $\text{MoO}(\text{O}_2)_2 \cdot 2\text{DMF}$ complex into the nanoporous CuBTC reacted with aminopyridine (Amp) and salicylaldehyde (Sal) compounds. The catalytic activity of the prepared catalyst in epoxidation of different olefins and allylic alcohols was assessed. The obtained catalyst demonstrated high catalytic efficiency due to the high molybdenum loading.

Experimental

General remarks

All reagents were purchased from Merck and Aldrich. Molybdenum(VI) oxodiperoxo complex, $\text{MoO}(\text{O}_2)_2 \cdot 2\text{DMF}$, was prepared according to the procedure reported in the literature [28]. Fourier transform infrared (FT-IR) spectra of the materials were obtained as KBr pellets on Perkin-Elmer Spectrum RXI FT-IR spectrometer. Powder X-ray diffraction (XRD) patterns were recorded on a PW1800 diffractometer using $\text{Cu K}\alpha$ radiation in the 2θ range of $4\text{--}60^\circ$ ($\lambda=1.5406 \text{ \AA}$). The metal content of the samples was estimated using a Contraa 700 atomic absorption spectrometer. The surface morphology and particle size of the materials were obtained on a ZEISS-FOS-UT scanning electron microscope (SEM). The surface area, pore volume and pore size distribution of the samples were determined by Nitrogen adsorption/desorption at liquid nitrogen temperature using Quantachrome Nova 2200e, Version 7.11 analyzer. Before the adsorption experiments, the samples were degassed under high vacuum at 120°C for 24 h. Nitrogen content of the modified materials was determined with a Thermo Finnigan (Flash 1112 Series EA) CHN Analyzer. Thermogravimetric analysis (TGA) measurement was performed using a TGA Q 50 Instrument. The samples were heated under argon atmosphere with a heating rate of $20^\circ \text{C min}^{-1}$. The oxidation products were analyzed using a gas chromatograph (HP, Agilent 68909N) equipped with a capillary column (HP-5) and a flame ionization detector (FID). Gas chromatography-mass spectrometry (GC-MS) was recorded using a Shimadzu-14A fitted with a capillary column (CBP5-M25).

PSM of the CuBTC MOF

CuBTC. $n\text{H}_2\text{O}$ MOF was synthesized through the previously reported hydrothermal method [29].

In a typical synthesis, 0.42 g (2.0 mmol) of H_3BTC was dissolved in 12 ml ethanol and then added to an aqueous solution (12 ml) of $\text{Cu}(\text{NO}_3)_2 \cdot 3\text{H}_2\text{O}$ (0.875 g, 3.6 mmol). The mixture was transferred to a Teflon-lined steel autoclave and heated at 120°C for 12 h. The obtained blue crystals were isolated by filtration and washed with deionized water and ethanol. The isolated material (0.5 g) was first activated at 150°C for 24 h to obtain dehydrated sample.

Modification of the CuBTC MOF was carried out as follows: dehydrated CuBTC (0.5 g) was suspended in 15 ml toluene and a solution of 4-aminopyridine (50 mg, 0.53 mmol) in dichloromethane was then added to the CuBTC suspension. The resulted mixture was refluxed for 16 h. The aminopyridine functionalized CuBTC (Amp-CuBTC) was collected by filtration and finally dried at 100°C for 3 h.

The prepared material (Amp-CuBTC) was then reacted with salicylaldehyde to yield the supported Schiff base ligand. As a general procedure, 0.5 g of Amp-CuBTC was diluted with 0.5 ml of salicylaldehyde in 10 ml chloroform and the mixture was refluxed for 16 h to give Sal-Amp-CuBTC material. The obtained solid was filtered, washed with chloroform and dried at 100°C for 3 h.

To prepare the supported molybdenum catalyst (Mo-Sal-Amp-CuBTC), $\text{MoO}(\text{O}_2)_2 \cdot 2\text{DMF}$ (0.05 mmol) was dissolved in dichloromethane (5 ml) and added to Sal-Amp-CuBTC (200 mg)

suspended in dichloromethane (10 ml). After refluxing the mixture for 4 h, the modified material was filtered and soxhlet extracted with dichloromethane for 24 h to remove the unreacted complex. The obtained catalyst was dried at 100°C for 3 h.

Catalytic epoxidation of olefins and allylic alcohols using Mo-Sal-Amp-CuBTC catalyst

As a typical procedure, the epoxidation reaction was carried out as follows: 14.4 mmol *Tert*-butyl hydroperoxide (TBHP, 80% in di-tertiary butyl peroxide) or hydrogen peroxide (H_2O_2 , 30% in water) as oxidant was added to a mixture of catalyst (100 mg) and olefin (8 mmol) in solvent (10 ml). The mixture was refluxed for appropriate time and the final products were quantified with isooctane (8.75 mmol) as internal standard.

Results and discussion

PSM of the CuBTC MOF

CuBTC is a nanoporous MOF decorated with unsaturated Cu^{2+} sites which are available to undergo chemical modification. CuBTC functionalization was conducted by the covalent attachment of 4-aminopyridine to the free metal sites created after dehydration followed by the addition of salicylaldehyde groups. In the final step, to achieve the molybdenum containing catalyst, reaction of the supported Schiff base ligand with the $\text{MoO}(\text{O}_2)_2 \cdot 2\text{DMF}$ complex resulted in the covalent attachment of the molybdenum complex. The schematic illustration is shown in Fig. 1.

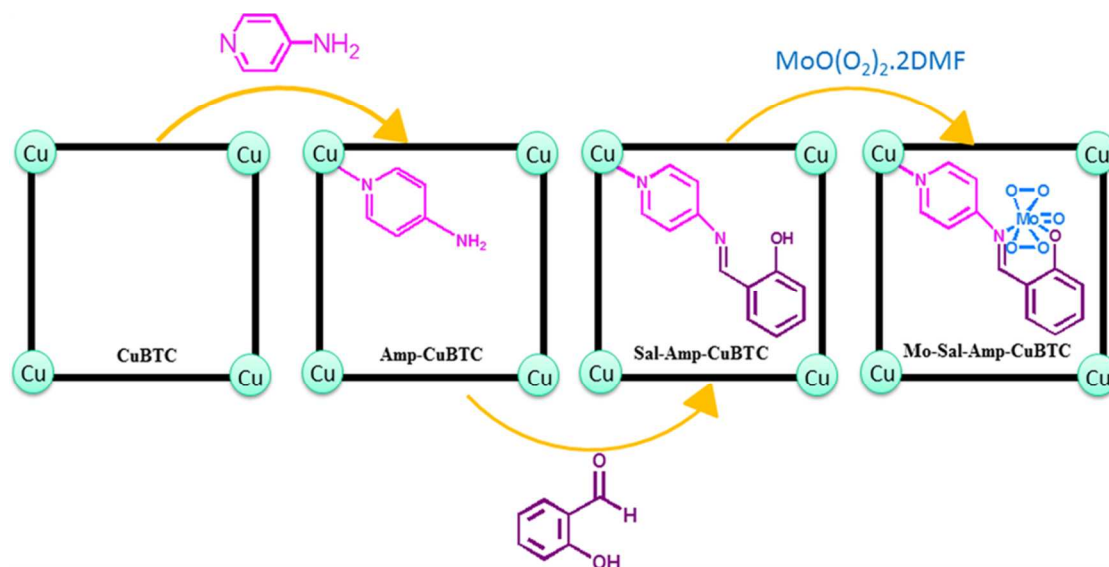


Fig. 1 The schematic representation of the modified CuBTC MOF.

Characterization of the modified CuBTC MOFs

The FT-IR spectra of the samples were employed to prove the CuBTC modification with different functionalities (Fig 2). In the FT-IR spectrum of the Amp-CuBTC (Fig. 2b), the characteristic band for the C=N group within the pyridine ring appeared at 1617 cm^{-1} . Furthermore, the band at 3364 cm^{-1} can be assigned to the N-H symmetric stretching vibration of 4-aminopyridine. After treatment of 4-aminopyridine groups with salicylaldehyde, a new band was appeared at 1647 cm^{-1} due to C=N vibration of the resulted bidentate Schiff base ligand (Fig. 2c). Also, the appearance of an adjacent band at 980 cm^{-1} proved the existence of Mo=O group and successful attachment of the molybdenum complex into the supported catalyst (Fig. 2d).

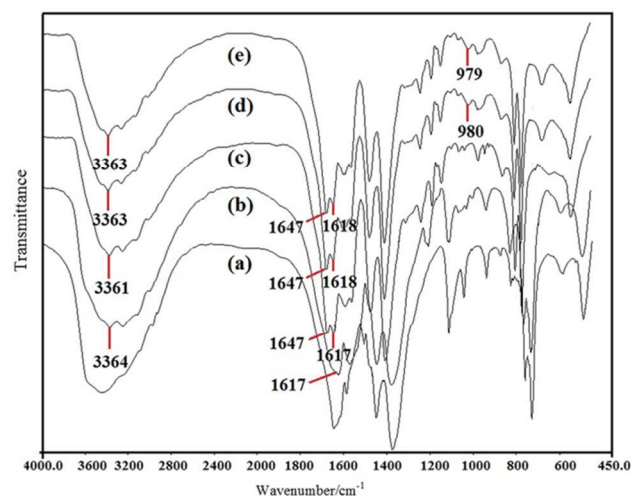


Fig. 2 FT-IR spectra of (a) CuBTC, (b) Amp-CuBTC, (c) Sal-Amp-CuBTC (d) Mo-Sal-Amp-CuBTC, (e) recycled Mo-Sal-Amp-CuBTC.

Chemical modification of the CuBTC MOF was also supported by atomic absorption spectroscopy (Cu: 28.65%, Mo: 3.74 %, 0.39 mmol g^{-1}) and CHN analyses. (Amp-CuBTC: C, 30.68; H, 2.56; N, 2.63%; Sal-Amp-CuBTC: C, 33.61; H, 2.11; N, 2.44%; Mo-Sal-Amp-CuBTC: C, 30.80; H, 2.14; N, 2.41%; %).

In order to confirm the phase purity and crystallinity of the bulk samples, powder X-ray diffraction measurements were taken. The patterns of the synthesized CuBTC before modification were in accordance with the simulated one, indicating that the desired material was obtained (Fig. 3b). Comparison of the powder X-ray diffraction patterns of the CuBTC MOF and the modified sample with the molybdenum complex (Fig. 3c) revealed a shift for all peaks to smaller 2θ angles during the modification process. This behavior represents the expansion of the framework depending on the guest molecules inside the pores. This peak shift clearly confirms the successful PSM of the framework. Furthermore, the modification of the CuBTC caused a decrease in the intensity of the peaks in the XRD patterns.

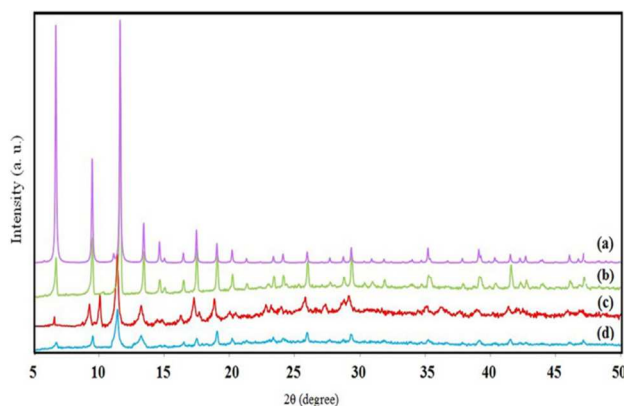


Fig. 3 XRD patterns of (a) simulated CuBTC, (b) as-synthesized CuBTC, (c) Mo-Sal-Amp-CuBTC, (d) recycled Mo-Sal-Amp-CuBTC.

SEM image of the Mo-Sal-Amp-CuBTC material as well as the as-synthesized CuBTC is depicted in Fig. 4. As can be seen in Fig. 4a, the SEM image of the as-synthesized CuBTC shows well-defined octahedral crystals with particle sizes between 4 and 10 μm . The PSM process of the CuBTC MOF led to a disruption of some particles (Fig. 4b). The SEM image of the Mo-Sal-Amp-CuBTC material reflects the effect of the treatments conducted on the CuBTC.

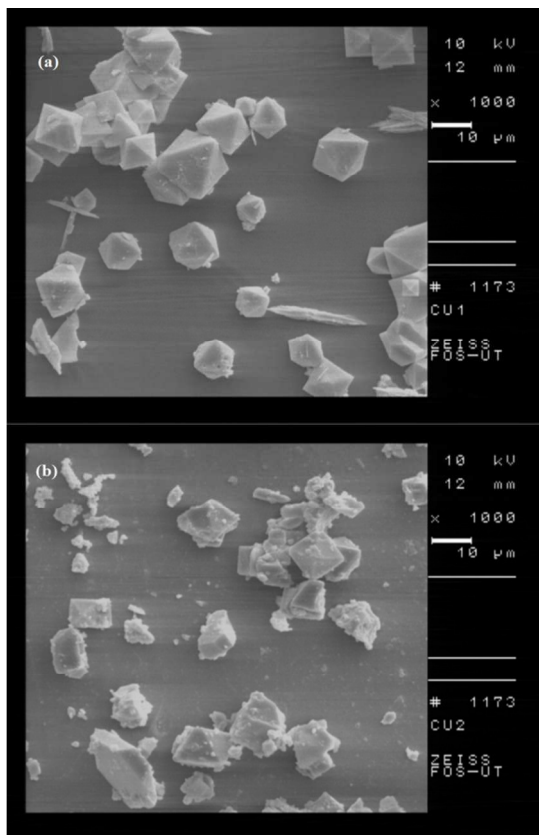


Fig. 4 SEM images of (a) as-synthesized CuBTC, (b) Mo-Sal-Amp-CuBTC.

In order to investigate the thermal behavior of the samples, thermogravimetric analysis was conducted. The TGA curve (Fig. 5a) demonstrates that upon heating, the as-synthesized CuBTC showed the first weight loss of about 34% up to 290 $^{\circ}\text{C}$ which was ascribed to the loss of surface and inner water molecules of the CuBTC framework. The second weight loss above 290 $^{\circ}\text{C}$ was attributed to the complete collapse of the CuBTC framework. In the TGA curve of the Mo-Sal-Amp-CuBTC catalyst (Fig. 5b), the first weight loss of only 7% was observed up to 110 $^{\circ}\text{C}$ because of water molecules replacement in CuBTC by aminopyridine linkers in the modified catalyst. Upon further heating, the TGA curve shows a large weight loss of about 43% between 110 to 450 $^{\circ}\text{C}$ which corresponds to the decomposition of the molybdenum Schiff base attached to the copper centers through PSM together with the BTC linkers of the framework.

Textural properties of the as-synthesized and modified CuBTC MOFs were determined with low temperature N_2 adsorption/desorption analyses (Fig. 6). In the adsorption isotherm of the as-synthesized CuBTC (Fig. 6a), the uptake of N_2 is increased

at low relative pressure and exhibits type I/IV mixed isotherm with a hysteresis loop created by the aggregated particles. The observed isotherm reflects the presence of both micropores and mesopores in the CuBTC MOF.

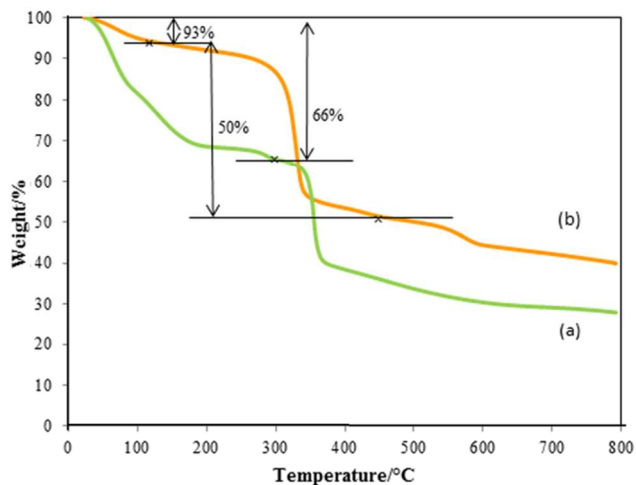


Fig. 5 TGA curves of (a) CuBTC, (b) Mo-Sal-Amp-CuBTC.

The modified CuBTC MOF (Mo-Sal-Amp-CuBTC) exhibited a similar isotherm (type I/IV) to the as-synthesized CuBTC MOF (Fig. 6b). However, the Mo-Sal-Amp-CuBTC catalyst shows a significant decrease in the Brunauer-Emmett-Teller surface area (S_{BET}) and total pore volume compared with the unmodified CuBTC MOF. The textural parameters of the unmodified and modified CuBTC are collected in Table 1. The as-synthesized CuBTC demonstrates a BET surface area and a total pore volume of $861 \text{ m}^2 \text{ g}^{-1}$ and 0.538 ml g^{-1} respectively. However, the Mo-Sal-Amp-CuBTC catalyst shows a significant decrease in these values ($62 \text{ m}^2 \text{ g}^{-1}$ and 0.088 ml g^{-1}). These observations clearly confirmed the presence of molybdenum Schiff base complex tethered within the pores of the MOF.

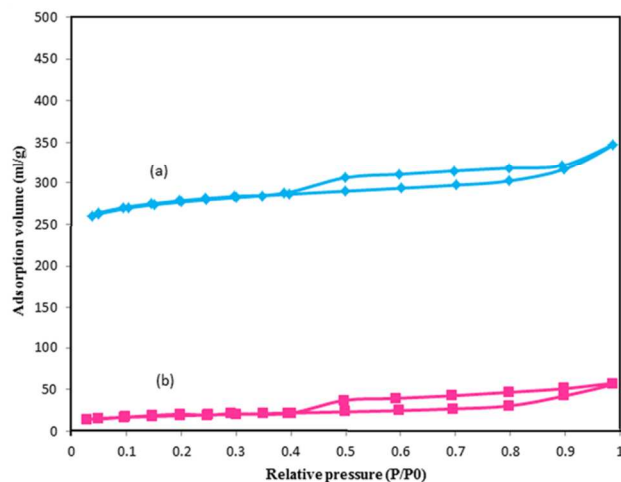


Fig. 6 Nitrogen sorption isotherms of (a) CuBTC, (b) Mo-Sal-Amp-CuBTC.

ARTICLE

Table 1 Texture parameters of the samples obtained from nitrogen sorption studies.

Sample	S_{BET} ($\text{m}^2 \text{g}^{-1}$)	$S_{\text{micro}}^{\text{a}}$ ($\text{m}^2 \text{g}^{-1}$)	V_{T}^{b} (ml g^{-1})	$V_{\text{micro}}^{\text{a}}$ (ml g^{-1})	$V_{\text{meso}}^{\text{c}}$ (ml g^{-1})
CuBTC	861	765	0.538	0.389	0.149
Mo-Sal-Amp-CuBTC	62	30	0.088	0.015	0.073

^a Calculated by the t-method.^b Total pore volume at $p/p_0=0.98$.^c Obtained by subtracting the micropore volume from the total pore volume at $p/p_0=0.98$.**Catalytic activity studies**

Since it has been proved that molybdenum containing materials are highly active in epoxidation reactions, we applied the Mo-Sal-Amp-CuBTC catalyst in the selective epoxidation of different olefins and allylic alcohols.

The optimal reaction conditions of the epoxidation reaction were explored using 3-Methyl-2-buten-1-ol as substrate in the presence of different solvents and oxidants. In the presence of TBHP as oxidant, Mo-Sal-Amp-CuBTC is more active in CH_2Cl_2 and CHCl_3 rather than CH_3CN , CH_3OH and $\text{C}_2\text{H}_5\text{OH}$ as solvents (Table 2). This observation can be explained with the increasing coordination ability as $\text{CH}_3\text{OH} \sim \text{C}_2\text{H}_5\text{OH} > \text{CH}_3\text{CN} > \text{CH}_2\text{Cl}_2 > \text{CHCl}_3$ and their competition with the oxygen molecule to occupy the coordination

sites of the catalyst. The obtained results are in good agreement with the previous report for coordination ability of donor strength scale [30]. Furthermore, when H_2O_2 was utilized as oxidant, the desired results were not obtained. However, with H_2O_2 as oxidant higher conversion was obtained for the epoxidation of 3-Methyl-2-buten-1-ol in CH_3CN compared to the other solvents. This may be due to the better miscibility of the reactants in this solvent. These observations are consistent with previous studies [25, 31]. According to the obtained results, the use of TBHP as oxidant and CHCl_3 as solvent resulted in more reactivity of the catalyst and hence the epoxidation reaction for other substrates was performed in this optimal reaction conditions.

Table 2 The screening oxidant and solvent nature for the epoxidation of 3-Methyl-2-buten-1-ol using Mo-Sal-Amp-CuBTC as catalyst.

Entry	Oxidant	Solvent	Time (h)	Conversion ^a (%)	Selectivity ^b (%)
1	TBHP	CHCl_3	1	99	>99
2		CH_2Cl_2	1	95	>99
3		CH_3CN	1	62	>99
4		CH_3OH	1	32	>99
5		$\text{C}_2\text{H}_5\text{OH}$	1	35	>99
6	H_2O_2	CHCl_3	1	40	>99
7		CH_2Cl_2	1	37	>99
8		CH_3CN	1	56	>99
9		CH_3OH	1	No reaction	-
10		$\text{C}_2\text{H}_5\text{OH}$	1	No reaction	-

Reaction conditions: catalyst (100 mg), 3-Methyl-2-buten-1-ol (8 mmol), oxidant (14.4 mmol), refluxing solvent (10 ml).

^a GC yield based on starting substrate.

^b Selectivity toward the formation of epoxide determined by GC-Mass or injection of reference.

In order to evaluate the efficiency of the prepared molybdenum catalyst, epoxidation of cyclooctene was tested in the presence of CuBTC, Amp-CuBTC, Sal-Amp-CuBTC and Mo-Sal-Amp-CuBTC as catalysts. As can be seen from Fig. 7, when Mo-Sal-Amp-CuBTC was applied as catalyst, the catalytic activity toward the formation of epoxide is clearly higher than that of other catalysts with only the copper centers as the active component. The catalytic activity of the Amp-CuBTC and Sal-Amp-CuBTC catalysts are similar to each other and slightly lower than the unmodified CuBTC MOF which may be due to the occupation of copper centers with aminopyridine groups. Similar to the Mo-Sal-Amp-CuBTC catalyst, MoO(O₂)₂.2DMF complex also showed high catalytic activity in the epoxidation of cyclooctene. Therefore, it can be concluded that the high catalytic efficiency of the catalyst is mainly due to the presence of the molybdenum complex. Although, CuBTC has been used as heterogeneous catalyst in oxidation reactions [32-33], PSM process enhances catalytic efficiency of the CuBTC framework. Similar results were also observed in a recently published paper [34]. In this report incorporation of dioxomolybdenum(VI) complex in a Zr^{IV}-based MOF resulted in increasing the catalytic activity of the modified framework compared to the unmodified one.

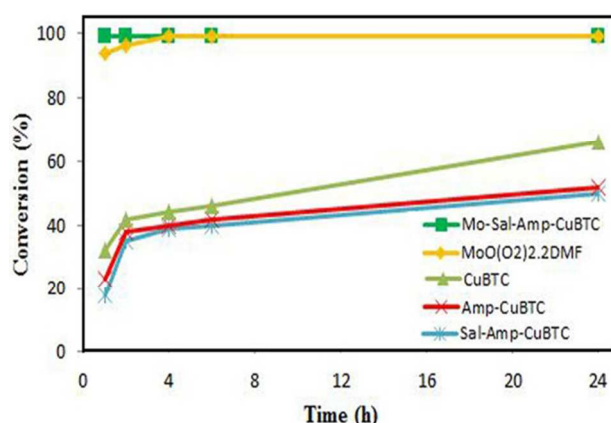


Fig. 7 Cyclooctene epoxidation in the presence of different catalysts.

In addition, to clarify the general applicability of the supported molybdenum catalyst, various substrates were subjected to the epoxidation reaction and the results are summarized in Table 3.

Table 3 Catalytic epoxidation of olefins and allylic alcohols using Mo-Sal-Amp-CuBTC catalyst.

Entry	Substrate	Time (h)	Conversion ^a (%)	Selectivity ^b (%)
1	Cyclooctene	1	99	>99
2	Cyclohexene	1	87	>99
3	Styrene	1	99	>99
4	Norbornene	1	95	>99
5	1-Octene	2	68	>99
6	1-Hexene	2	74	>99
7	<i>trans</i> -Stilbene	2	62	>99

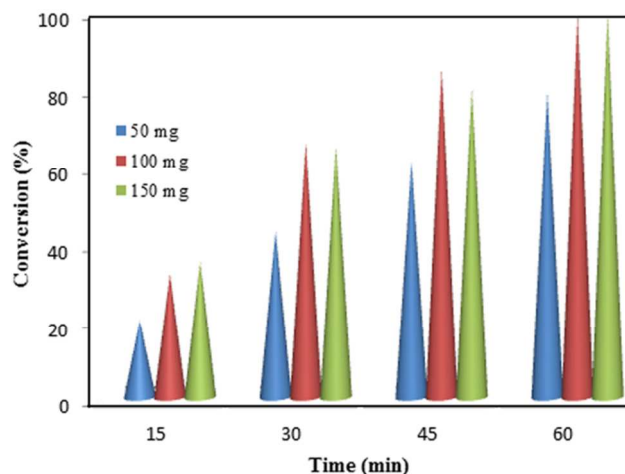


Fig. 8 The screening of catalyst amount for the epoxidation of 3-Methyl-2-buten-1-ol using Mo-Sal-Amp-CuBTC catalyst.

The resultant conversions revealed the high catalytic activity of the synthesized material. Furthermore, the high reactivity of the allylic alcohols is probably owing to the participation of hydroxyl group in approaching the double bond to the electrophilic oxygen center of the oxidant. It is expected that olefins with higher electron density of the double bonds show more epoxidation reactivity. Hence, the reaction rates for cyclooctene and cyclohexene with double bond driven from secondary carbons are higher than reactivity of 1-octene and 1-hexene.

The effect of the catalyst amount on the epoxidation of 3-Methyl-2-buten-1-ol has been shown in Fig. 8. It is clear that substrate conversion increases with higher amount of catalyst up to 100 mg beyond which no considerable oxidation occurs.

The recyclability of the Mo-Sal-Amp-CuBTC catalyst was examined in the epoxidation of 3-Methyl-2-buten-1-ol and cyclohexene. After the first catalytic run, the catalyst was separated from the reaction mixture by filtration, thoroughly washed with ethanol and then used directly for the subsequent runs under the same reaction conditions. The results included in Fig. 9 indicate that the recovered catalyst maintained similar activity after four cycles.

8	<i>cis</i> -Stilbene	2	70	>99
9	3-Methyl-2-buten-1-ol	1	99	>99
10	Allyl alcohol	1	99	>99
11	1-Octen-3-ol	2	85	>99

Reaction conditions: catalyst (100 mg), olefins (8 mmol), TBHP (14.4 mmol), refluxing chloroform (10 ml).

^a GC yield based on starting substrate.

^b Selectivity toward the formation of epoxide determined by GC-Mass or injection of reference.

These observations were in accordance with atomic absorption spectroscopy analysis for which no significant loss of molybdenum was observed after subsequent four runs (Molybdenum: 0.36 mmol g⁻¹). To further investigate the stability of the catalyst, FT-IR and XRD analyses were applied. The similarity of the FT-IR spectrum and XRD patterns of the recycled and fresh catalyst clearly demonstrates the catalyst stability under the reaction conditions (Fig. 2e and 3d). In order to clarify the possible catalytic contribution of the solubilized molybdenum species, a hot filtration test was performed. Therefore, in a separate test with cyclohexene, the liquid phase of the reaction mixture was collected by filtration after 2 h of the reaction and then the filtrate left to react for a further 24 h. The cyclohexene conversion reached 89% after 24 h, suggesting that the epoxidation reaction do not proceed after the catalyst filtration. On the basis of these observations, it can be concluded that the epoxidation reaction is truly heterogeneous in nature and there are no significant molybdenum species in the solution.

A comparison of the prepared catalyst with related modified MOFs (MOFs modified with different molybdenum complexes) is given in Table 4. The higher catalytic activity of the supported molybdenum complexes on the CuBTC MOF can be concluded from these data.

The results obtained by this catalytic system were also compared with previously reported oxodiperoxo molybdenum catalysts derived from different solid supports (Table 5). In an attempt to develop a novel heterogeneous molybdenum catalyst, immobilization of oxodiperoxo molybdenum complex onto Si-MCM-41 and Al-MCM-41 with a bidentate 2-[3(5)-pyrazolyl]pyridines ligand was achieved [8]. The obtained catalysts were applied in heterogeneous epoxidation of cyclooctene (Table 5, entry 1 and 2). Silica coated

magnetic nanoparticles were also utilized to prepare supported oxodiperoxo molybdenum catalyst [6]. The higher catalytic activity of the Mo-Sal-Amp-CuBTC catalyst is related to the CuBTC MOF as support that can act as a promoter in the catalytic reaction. Although the main catalytic activity of the obtained catalyst is due to the presence of molybdenum complex, CuBTC with free coordination Cu(II) enhanced the catalytic activity of the Mo-Sal-Amp-CuBTC catalyst.

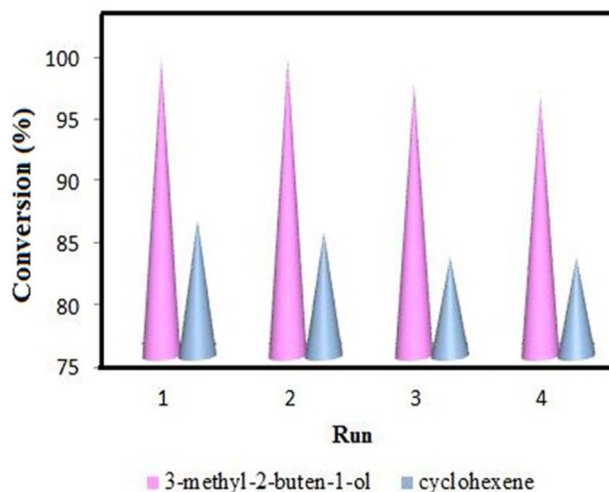


Fig. 9 Recyclability of the Mo-Sal-Amp-CuBTC catalyst.

Table 4 Comparison of the results obtained for epoxidation of cyclohexene catalyzed by different molybdenum-based MOFs.

Entry	Catalyst	Reaction conditions	Time (h)	Conversion (%)	Reference
1	UiO-66-sal-MoD	0.5 mmol cyclohexene, 2 mmol TBHP, 5 ml CH ₃ CN, 40 mg catalyst	24	70	22
2	Mo@COMOC-4	25 mmol cyclohexene, 9 ml TBHP, 30 ml chloroform	7	81	23
3	Mo-AMP-CuBTC	8 mmol cyclohexene, 14.4 mmol TBHP, 10 ml chloroform, 100 mg catalyst	2	90	25
4	Mo-Sal-Amp-CuBTC	8 mmol cyclohexene, 14.4 mmol TBHP, 10 ml chloroform, 100 mg catalyst	1	87	This work

Table 5 Comparison of the results obtained for epoxidation of cyclooctene catalyzed by supported oxodiperoxo molybdenum complex on different solid supports.

Entry	support	Reaction conditions	Time (h)	Conversion (%)	Reference
1	Si-MCM-41	9.07 mmol cyclooctene, 1.7 ml TBHP 5.5 M, 25 ml CHCl ₃ , 100 mg catalyst	7	85	8
2	Al-MCM-41	9.07 mmol cyclooctene, 1.7 ml TBHP 5.5 M, 25 ml CHCl ₃ , 100 mg catalyst	7	85	8
3	Silica coated Fe ₂ O ₃ nanoparticle	1 mmol cyclooctene, 1.2 mmol TBHP, 5 ml chloroform	6	96	6
4	Mo-Sal-Amp-CuBTC	8 mmol cyclooctene, 14.4 mmol TBHP, 10 ml chloroform, 100 mg catalyst	1	99	This work

Conclusion

In the present work, we have succeeded in designing a new heterogeneous oxodiperoxo molybdenum catalyst using Cu₃(BTC)₂ metal organic framework as solid support. Modification of the Cu₃(BTC)₂ metal organic framework was successfully conducted by immobilization of the molybdenum Schiff base complex into the nanopores of the framework. The catalytic activity of the prepared catalyst was investigated in the epoxidation of different olefins and allylic alcohols. The functionalized Cu₃(BTC)₂ metal organic framework did not decompose during the modification process and even during the epoxidation reaction, indicating the high efficiency of the prepared catalyst.

Acknowledgments

The financial support from the University of Tehran is gratefully appreciated.

References

- M. Beller, C. Bolm, *Transition Metals for Fine Chemicals and Organic Synthesis*, Wiley-VCH, Weinheim, 1998, vol.2, pp. 261-266.
- S. Campestrini, F. Di Furia, P. Rossi, A. Torboli, G. Valle, *J. Mol. Catal.*, 1993, **83**, 95-105.
- K. A. Joergensen, *Chem. Rev.*, 1989, **89**, 431-458.
- W. R. Thiel, T. Priermeier, *Angew. Int. Ed. Engl.*, 1995, **34**, 1737-1738.
- M. Amini, M. M. Haghdoost, M. Bagherzadeh, *Coord. Chem. Rev.*, 2013, **257**, 1093-1121.
- S. Shylesh, J. Schweizer, S. Demeshko, V. Schünemann, S. Ernst, W.R. Thiel, *Adv. Synth. Catal.*, 2009, **351**, 1789 - 1795.
- M. Jia, W.R. Thiel, *Chem. Commun.*, 2002, 2392-2393.
- M. Jia, A. Seifert, W.R. Thiel, *Chem. Mater.*, 2003, **15**, 2174-2180.
- M. Jia, A. Seifert, M. Berger, H. Giegengack, S. Schulze, W.R. Thiel, *Chem. Mater.*, 2004, **16**, 877-882.
- M. Jia, A. Seifert, W.R. Thiel, *J. Catal.*, 2004, **221**, 319-324.
- M. R. Maurya, M. Kumar, S. Sikarwar, *React. Funct. Polym.*, 2006, **66**, 808-818.
- U. Ravon, M. E. Domine, C. Gaudillère, A. Desmartin-Chomel, D. Farrusseng, *New J. Chem.*, 2008, **32**, 937-940.
- A. Corma, H. García, F. X. Llabrés i Xamena, *Chem. Rev.*, 2010, **110**, 4606-4655.
- J. Y. Lee, O. K. Farha, J. Roberts, K. A. Scheidt, S. T. Nguyen, J. T. Hupp, *Chem. Soc. Rev.*, 2009, **38**, 1450-1459.
- Zh. Wang, S. M. Cohen, *Chem. Soc. Rev.*, 2009, **38**, 1315-1329.
- S. M. Cohen, *Chem. Rev.*, 2012, **112**, 970-1000.
- C. Janiak, J. K. Vieth, *New J. Chem.*, 2010, **34**, 2366-2388.
- Zh. Sun, G. Li, H. -O. Liu, L. Liu, *Appl. Catal., A: Gen.*, 2013, **466**, 98-104.
- F. Zadehahmadi, Sh. Tangestaninejad, M. Moghadam, V. Mirkhani, I. Mohammadpoor-Baltork, A. R. Khosropour, R. Kardanpour, *Appl. Catal., A: Gen.*, 2014, **477**, 34-41.
- M. J. Ingleson, J. P. Barrio, J. -B. Guilbaud, Y. Z. Khimyak, M. J. Rosseinsky, *Chem. Commun.*, 2008, 2680-2682.
- S. Bhattacharjee, D. -A. Yang, W. -S. Ahn, *Chem. Commun.*, 2011, **47**, 3637-3639.
- J. Tang, W. Dong, G. Wang, Y. Yao, L. Cai, Y. Liu, X. Zhao, J. Xu, L. Tan, *RSC Adv.*, 2014, **4**, 42977-42982.
- K. Leus, Y. -Y. Liu, M. Meledina, S. Turner, G. Van Tendeloo, P. Van Der Voort, *J. Catal.*, 2014, **316**, 201-209.
- J. Kim, H. -Y. Cho, W. -S. Ahn, *Catal. Surv. Asia.*, 2012, **16**, 106-119.
- S. Abednatanzi, A. Abbasi, M. Masteri-Farahani, *J. Mol. Catal. A: Chem.*, 2015, **399**, 10-17.
- M. Masteri-Farahani, S. Abednatanzi, *Inorg. Chem. Commun.*, 2013, **37**, 39-42.
- M. Masteri-Farahani, S. Abednatanzi, *Appl. Catal., A: Gen.*, 2014, **478**, 211-218.
- H. Mimoun, I. Seree de Roch, L. Sajus, *Bull. Soc. Chim. Fr.*, 1969, 1481-1492.
- K. Schlichte, T. Kratzke, S. Kaskel, *Microporous Mesoporous Mater.*, 2004, **73**, 81-88.
- M. Sandström, I. Persson, P. Persson, *Acta. Chem. Scand.*, 1990, **44**, 653-675.
- M. Najafi, A. Abbasi, M. Masteri-Farahani, V. H. Rodrigues, *Inorg. Chem. Commun.*, 2014, **46**, 251-253.
- A. Dhakshinamoorthy, M. Alvaro, H. Garcia, *ACS Catal.*, 2011, **1**, 48-53.
- A. Dhakshinamoorthy, M. Alvaro, H. Garcia, *J. Catal.*, 2009, **267**, 1-4.
- P. Neves, A. C. Gomes, T. R. Amarante, F. A. Almeida, M. Pillinger, I. S. Goncalves, A. A. Valente, *Microporous Mesoporous Mater.*, 2015, **202**, 106-114.

Table of contents

Abstract.....	1
Introduction	1
Experimental	2
General remarks.....	2
PSM of the CuBTC MOF.....	2
Catalytic epoxidation of olefins and allylic alcohols using Mo-Sal-Amp-CuBTC catalyst.....	2
Results and discussion.....	2
PSM of the CuBTC MOF.....	2
Characterization of the modified CuBTC MOFs.....	3
Catalytic activity studies	5
Conclusion.....	8
Acknowledgments.....	8
References.....	8

Graphical abstract

A new bimetallic heterogeneous epoxidation catalyst was prepared through Chemical modification of $\text{Cu}_3(\text{BTC})_2$ metal organic framework.

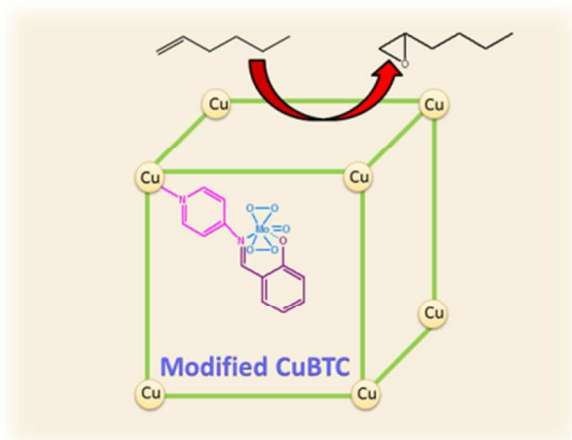
**Captions to graphics**

Fig. 1 The schematic representation of the modified CuBTC MOF.

Fig. 2 FT-IR spectra of (a) CuBTC, (b) Amp-CuBTC, (c) Sal-Amp-CuBTC (d) Mo-Sal-Amp-CuBTC, (e) recycled Mo-Sal-Amp-CuBTC.

Fig. 3 XRD patterns of (a) simulated CuBTC, (b) as-synthesized CuBTC, (c) Mo-Sal-Amp-CuBTC, (d) recycled Mo-Sal-Amp-CuBTC.

Fig. 4 SEM images of (a) as-synthesized CuBTC, (b) Mo-Sal-Amp-CuBTC.

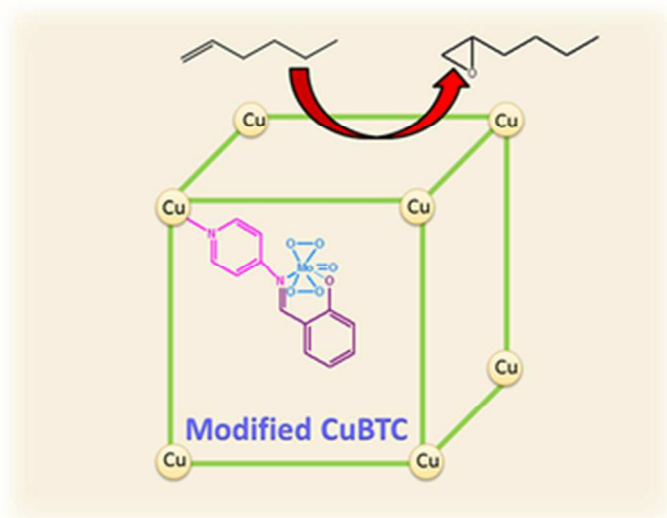
Fig. 5 TGA curves of (a) CuBTC, (b) Mo-Sal-Amp-CuBTC.

Fig. 6 Nitrogen sorption isotherms of (a) CuBTC, (b) Mo-Sal-Amp-CuBTC.

Fig. 7 Cyclooctene epoxidation in the presence of different catalysts.

Fig. 8 The screening of catalyst amount for the epoxidation of 3-Methyl-2-buten-1-ol using Mo-Sal-Amp-CuBTC catalyst.

Fig. 9 Recyclability of the Mo-Sal-Amp-CuBTC catalyst.



29x23mm (300 x 300 DPI)